Journal of Zhejiang University-SCIENCE A (Applied Physics & Engineering)
ISSN 1673-565X (Print); ISSN 1862-1775 (Online)
www.zju.edu.cn/jzus; www.springerlink.com
E-mail: jzus@zju.edu.cn

Surface settlement caused by twin-parallel shield tunnelling in sandy cobble strata*

Chuan HE†[1,2], Kun FENG[1,2], Yong FANG[1,2], Ying-chao JIANG[1,2]

([1]*MOE Key Laboratory of Transportation Tunnel Engineering, Southwest Jiaotong University, Chengdu 610031, China*)

([2]*School of Civil Engineering, Southwest Jiaotong University, Chengdu 610031, China*)

†E-mail: chuanhe21@163.com

Received Sept. 27, 2012; Revision accepted Oct. 10, 2012; Crosschecked Sept. 27, 2012

Abstract: City metro tunnels are usually constructed as twin-parallel tunnels and their adjacent construction may lead to surface deformation, affecting the surface environment and the safety of the tunnels. Due to its strong dispersion, sandy cobble strata can be easily disturbed by shield tunneling. Based on the project of the Chengdu Metro Line 1, field and model tests were carried out to study the surface settlement caused by shield tunneling in sandy cobble strata by measuring surface settlement curves, ground loss ratios and construction influence zones. The discrete element method (DEM) was used to study the factors affecting the formation of ground arches in sandy cobble strata at the microscopic level. Results show that the shape of the surface settlement curve in sandy cobble strata is different from that in soft soil. The buried depth and clear spacing of the two tunnels had a significant impact on the formation of ground arches.

Key words: Twin-parallel shield tunneling, Surface settlement, Ground loss, Field test, Discrete element method (DEM), Model test

doi:10.1631/jzus.A12ISGT6 **Document code:** A **CLC number:** U45

1 Introduction

Shield tunneling has become the main method for the construction of urban tunnels in China (Chen *et al.*, 2009). The method inevitably generates disturbance of the surrounding soil, causing ground deformation. Ground loss, which is the main factor causing ground settlement, is usually taken to characterize the soil disturbance caused by shield construction.

Based on a large number of field test results of ground surface settlement during tunnel excavation, Peck (1969) first proposed the concept of ground loss and a practical method to estimate surface settlement. In his view, the volume of the settling trough caused by tunnel excavation should be equal to the volume of ground loss under undrained conditions. A theoretical formula to predict the curve of ground settlement was proposed based on the assumptions that the ground loss is uniformly distributed along the tunnel length, and the lateral surface settlement is distributed normally. To take the impact of the ground loss into consideration, the 2D equivalent gap around the tunnel was defined and incorporated into the theoretical model by Rowe and Lo (1983) and Lo and Ng (1984). The gap was determined based on the 3D movements into the face, the shape of the shield machine, overcutting caused by the pitching and yawing of the tunnelling machine, the soil type, the tunneling machine, lining diameters, and the consolidation of any disturbed or remoulded regions around the tunnel. Sagaseta (1987; 1988; 1989) introduced the mirror source method and ground loss parameters, and proposed a calculation formula to predict surface settlement. Loganathan and Poulos

* Project supported by the National Basic Research (973) Program of China (No. 2010CB732105), and the National Natural Science Foundation of China (Nos. 50908193, 50925830, and 51208432).

(1998) considered that, due to the deformation of the segments and the movement of the tunnel face, the shape of the gap around the shield machine is actually an oval. Thus, the traditional ground loss parameter was redefined as equivalent ground loss. The concept of gap parameters was put forward by Lee (1992), and a calculation formula of equivalent ground loss based on an analytical solution was worked out by Verruijt and Booker (1996).

To explore the characteristics of ground deformation caused by ground loss, O'Reilly and New (1982) collected and analyzed the largest settlement section area of the settling trough and the position of the inflection point of 19 tunneling cases in cohesive soil strata and 16 tunneling cases in sandy soil in Britain. The results showed that the ground settlement caused by tunneling was not related to the construction methods or tunnel diameters.

Based on the uniform ground movement model, Wei (2007; 2009a; 2009b; 2010) derived a 2D solution of ground deformation caused by ground loss during shield construction using the formula of Loganathan (1998). Meanwhile, based on measurements of surface settlement and ground loss ratios during shield tunneling at home and abroad, the relationships among the width of the settling trough, tunnel depth and diameter and other parameters in cohesive soil strata were described, and a method to determine ground loss ratios in the shield construction process was proposed.

Sandy cobble strata are significantly discrete. Ground settlement caused by shield construction in such strata is different from that in continuous media such as cohesive soils. Previous studies of ground disturbance from shield tunneling were carried out mainly in continuous media such as adhesive clay. Few studies have dealt with discrete ground such as sandy cobble strata, and studies involving twin-parallel shield tunneling are especially rare. In this work, field and model tests were carried out, based on the Chengdu Metro Line 1, to study the surface settlement caused by twin-parallel shield tunnelling in sandy cobble strata. The ground loss ratio and the affected areas of surface settlement were measured. Furthermore, the mechanism of surface settlement and the effect of tunnel spacing on surface settlement were studied at the microscopic level using the discrete element method (DEM).

2 Field test

2.1 Project overview

The Chengdu Metro Line 1, which stretches for about 18.5 km underground, starts from Shengxianhu Station in the north of Chengdu, passes through the North Railway Station, and extends to Shijicheng Station in the south of the city. The tunnel benefits from an erosion-accumulation landform all the way. Groundwater within the region exists mainly in the form of pore water from the quaternary loose accumulation of sandy cobble and gravel layers. The entire line passes through the quaternary water-rich sandy cobble and gravel strata. The strata exhibit poor plastic flow and high permeability, poor cementation capacity, and high strength of single stones, and the cobble acts as a skeleton. The strata are extremely easily disturbed by ground loss during shield tunneling. So a number of monitoring points were set up along the shield axis to guide the tunneling process.

The surface settlement consists of time-history curves of surface settlement at the tunnel center axes of both the left and right lines and the surface settling trough. Monitoring was carried out using precise leveling in accordance with the Chinese national 2nd-class standard of measurement. The monitoring points were placed every 10 m along the axis of the shield tunnel, and every 5 m within important areas. The monitoring range was determined based on the tunnel depth. Highly precise levelings (DSZ2+FS1) and indium rulers were used for measurement to ensure an accuracy of ±1.0 mm.

According to the hydro geological conditions at the tunnel site and the construction schedule, the field testing was carried out from Tongzilin Station to South Railway Station. In this district, an earth pressure balanced (EPB) shield machine was employed tunneling south to north, starting from the South Railway Station. The diameter (D) of the shield machine was 6250 mm, and the body length (L) of shield was 7925 mm. Monitoring sections were selected at the K14+319, where the buried depth was about 11 m, and the shield machine would pass through the sandy cobble strata with a high groundwater head. The cobble, with particle size ranging from 20 to 200 mm, accounted for 55% to 80% of the strata, and erratic boulders accounted for 0 to 22.3%. The right lane was constructed first, and the spacing between the two lines was 7 m. A diagram of the geology and the

monitoring point layout is shown in Fig. 1. The physico-mechanical parameters are listed in Table 1.

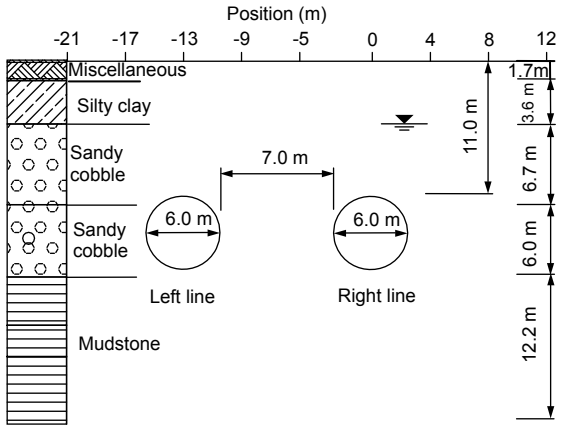

Fig. 1 Diagram of the test section showing the geology and the positions of monitoring points (unit: m)

Table 1 Physico-mechanical parameters

Stratum	γ (kN/m^3)	E (MPa)	v	φ (°)	c (kPa)
Miscellaneous	18.5	1.5	0.39	10	8
Silty clay	19.5	6.2	0.30	27	22
Sandy cobble	21.5	36.5	0.31	38	0
Mudstone	22.0	60.0	0.21	41	60

γ is the density, E is the Young's modulus, v is Poisson's ratio, φ is the internal friction angle, and c is the cohesion force

2.2 Test results

The surface settlement was measured when the cutter was 1D before the monitoring sections, below the monitoring sections, and 1D after the monitoring sections and above the shield tail after the cutter had passed through the monitoring section. The surface settlement curves of the left and right lines at different times are shown in Figs. 2 and 3. The surface settlements at different times are listed in Table 2.

Figs. 2a and 2b show that after the right line excavation, the surface settlement curve was "V" shaped. After the two lines were excavated, the surface settlement curve was "W" shaped, as if the two single-line surface settlement curves had been superimposed. The results also convey the surface deformation mechanism at different times. Before the shield reached the monitoring sections, both sides of the ground surface were uplifted owing to the extrusion effect between the heading face and the ground. From when the cutter was below the monitoring sections to when the cutter was 1D past the monitoring sections, a shear sliding surface appeared because of the shear friction between the shield shell and the surrounding soil. The shear force develops in the soil around the sliding surface, and further causes the surface settlement to increase. After the shield tail passed through the monitoring sections, the surface settlement caused by ground loss continued to increase because the gap between the soil and the tunnel was not filled immediately with grouting or because the grouting effect had not worked in time. Surface settlement at different stages accounted for more than 20% of the total settlement, and the settlement values of each stage showed little difference. These results indicate that ground settlement is sensitive to the shield tunneling process in sandy cobble strata, and that the cutting face pressure, the friction between the shield shell and surrounding soil, and the shield tail void can easily affect the surface settlement. In terms of the excavation time, the final settlement caused by left line tunneling was greater than that of the right line. That was due to the small spacing (about 1D) between the two tunnels. The surrounding soil was disturbed while the right line was under construction, and when the left tunnel was constructed, the secondary disturbance was superimposed on that of the left line and a larger settlement occurred.

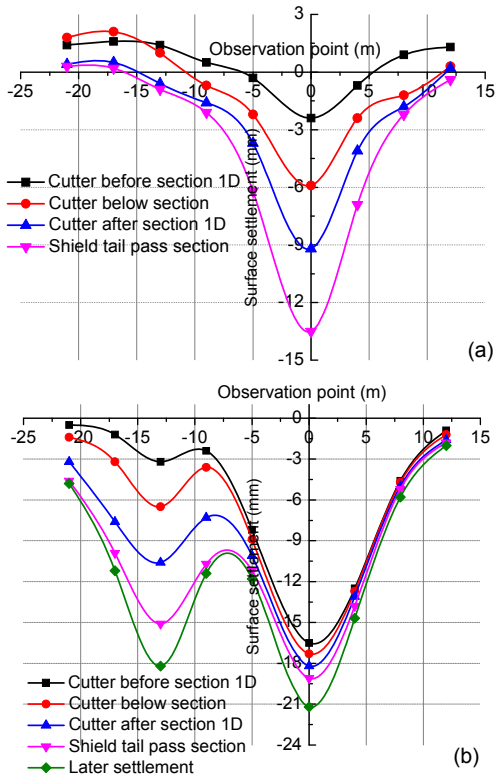

Fig. 2 Surface settlement curve of the right line (a) and left line (b) at different times

Table 2 Surface settlement at different times

	Stage	Phasic settlement (mm)	Cumulative settlement (mm)	Proportion of total settlement (%)
Right line first	1D before section	−2.4	−2.4	17.8
	At the section	−3.5	−5.9	26.0
	1D after section	−3.3	−9.2	24.4
	Past the section	−4.3	−13.5	31.8
Left line later	1D before section	−3.2	−3.2	21.2
	At the section	−3.3	−6.5	21.8
	1D after section	−4.1	−10.6	27.2
	Past the section	−4.5	−15.1	29.8
Later settlement (mm)		−18.2 (left line), −21.2 (right line)		

Fig. 3 shows the time-history curves of surface settlement during the right line excavation process. The surface settlement was split into three stages divided by two monitoring points: the point at which the shield reached the section and the point at which the shield tail passed the monitoring section. The gap between the shield and the tunnel was the main factor leading surface settlement in the sandy cobble strata. The surface settlement increased over time following ground loading and soil consolidation. The maximum surface settlement during the monitoring period was 18.2 mm (left line) and 21.2 mm (right line).

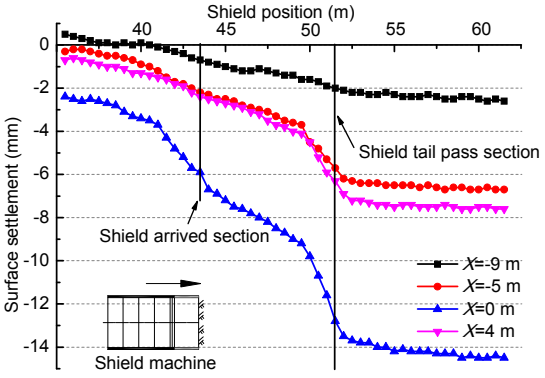

Fig. 3 Surface settlement time-history curve of the right line

3 Model test

Model testing is one of the most important test methods. Models can be used instead of prototype structures. Tests are usually based on a certain geometric, physical relationship. The results of model tests can be transformed into prototypes using similarity ratios. The EPB model shield machine was developed and manufactured on the basis of a geometry similarity ratio of 12:1 by the Department of Tunnel and Underground Engineering of the Southwest Jiaotong University, China. The prototype shield machine was used in the Chengdu Metro Line 1 project. Research on the influence of shield tunneling on ground settlement in sandy cobble strata was conducted based on a model test system of shield tunneling.

3.1 Model test system of shield tunneling

The model test system of shield tunneling was composed mainly of an EPB model shield machine, a test soil bin and a tunneling console (Fig. 4). The basic dimensions of the shield machine model included mainly its external diameter, inner diameter, the shield tail void, and the segment external diameter. The length of the shield machine had to meet the space requirements of equipment layout and the assembly of the segment. The shield machine was made of pure steel to simulate its rigid support against soil. The basic size of the model was 850 mm in length (including 100 mm between the cutter and the compartment, and the 750 mm shield tail), with an external diameter of 520 mm, an inner diameter of 508 mm, and a shield shell thickness of 6 mm.

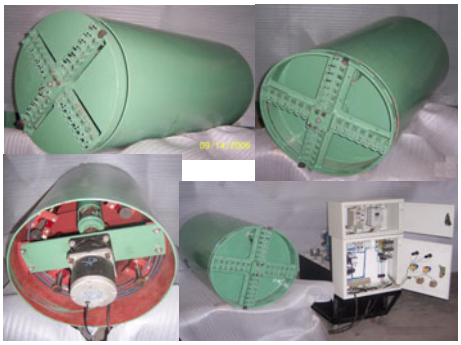

Fig. 4 EPB model shield machine and tunneling console

The model shield machine consisted mainly of a jacking system, a cutting system and a slag discharge system. The jacking system consisted of four jacks, each with a maximum thrust of 5 kN, placed equidistantly around the shield machine. The cutting system consisted of four main parts: a cutter head, main bearings, a stir bar and a cutter head motor. Two different types of cutter head were developed in order to suit different strata. The slag discharge system included a screw conveyor and a driving motor. Two kinds of screw conveyor were developed, a shaft type and a belt type. The model test adopted a board cutter head and a shaft slag discharge system to accommodate the need to tunnel in a sandy cobble stratum.

According to Saint-Venant's Principle and the distribution of ground stress of a circular tunnel, the influence of tunneling on ground stress is distributed mainly within a circle with a radius of from 3D to 5D around the tunnel, and affects mainly the stratum above the tunnel. Therefore, the main control boundaries were left, right and longitudinal boundaries. The longitudinal boundary was determined by the test scale and the tunneling length and had to fit the monitoring points during the whole process, including the points at which the shield machine reached, passed through and completed the tunnel. The final size of the test soil bin was 4400 mm wide, 4400 mm long and 3000 mm high, and the clear distance between the centers of the two tunnels was 520 mm (Fig. 5).

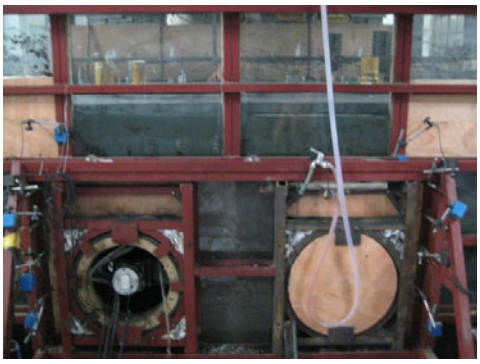

Fig. 5 Soil trough of the model test

3.2 Model test material

The physico-mechanical parameters of the actual stratum were selected according to the report of an engineering survey (Table 1). The materials of the model stratum were chosen according to the macro-mechanical properties of the actual stratum regardless of grain composition. Using the artificial synthetic materials with specific proportions of barite powder, river sand, fly ash and quartz sand, the mechanical parameters such as Young's modulus (E), density (γ), internal friction angle (φ) and cohesion force (c) of the model stratum were tested using direct shear tests and compression tests. The physico-mechanical parameters of the model test stratum are listed in Table 3.

Table 3 Physico-mechanical parameters of model test stratum

Stratum	E (MPa)	γ (kN/m^3)	φ (°)	c (kPa)
Actual	25–45	20–23	35–45	0
Model	3.5	20.8	33.25	7

The tunnel linings in the model test were made of four wooden segments each with a central angle of 90°. The external diameter and thickness of each segment were 500 mm and 50 mm, respectively. Considering the connection between segments and rings, and the grouting in the tunneling process, the grouting holes and connection bonds were set upon model segments. Because the large deformation of the model linings under formation pressure may cause increases in ground loss, a circular keeping device with an external diameter of 424 mm was developed, made of a Φ10 mm plain bar (Fig. 6).

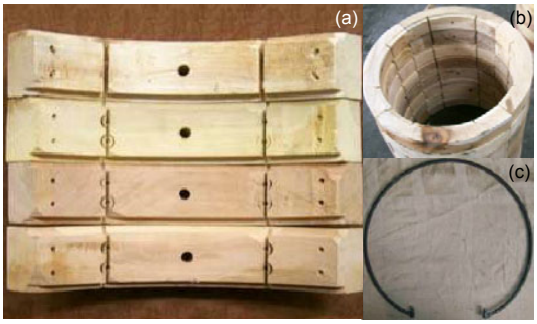

Fig. 6 Segment lining structure and circular keep unit
(a) Model segments; (b) Tunneling lining; (c) Circular keeping device

3.3 Model test content

The purpose of this test was to study the surface settlement curve of the twin-parallel shield tunnel in sandy cobble strata. Values of surface settlement at different stages were recorded at monitoring points placed in three sections (Fig. 7). There were seven monitoring points in each section with a distance of 520 mm between each two points in the transverse and longitudinal directions, so that the settlement curve of a cross-section and a time-history curve in the longitudinal direction could be tested. The displacement was measured using a displacement meter (SP-XB) with an accuracy of 0.001 mm.

3.4 Model test results analysis

The prototype results were transformed from the model test results according to the geometry similarity ratio of 1:12. The cases were selected to correspond with the field tests. Thus, the four cases tested included the cutter 1D before the monitoring sections, the cutter below the monitoring sections, the cutter 1D after the monitoring sections, and the shield tail through the monitoring sections.

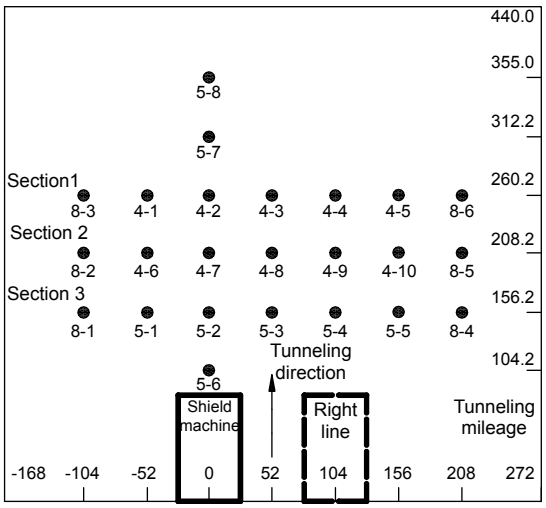

Fig. 7 Distribution of monitoring points (unit: cm)

Taking Section 2 as an example, the surface settlement curves of the left and right lines, and the time-history curve of the left line are shown in Figs. 8 and 9, respectively. In Figs. 8a and 8b, the origin of the coordinates is set to the center axis of the left tunnel, and the abscissa indicates the location of each monitoring point.

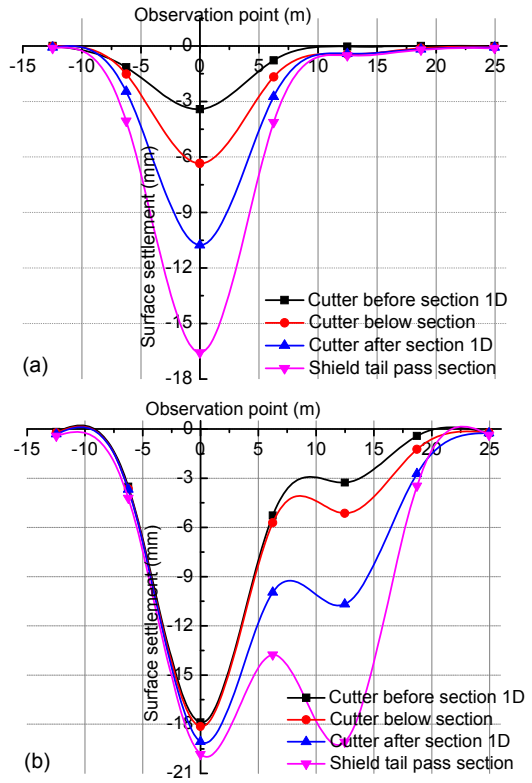

Fig. 8 Section 2 surface settlement curve of the left line (a) and right line (b)

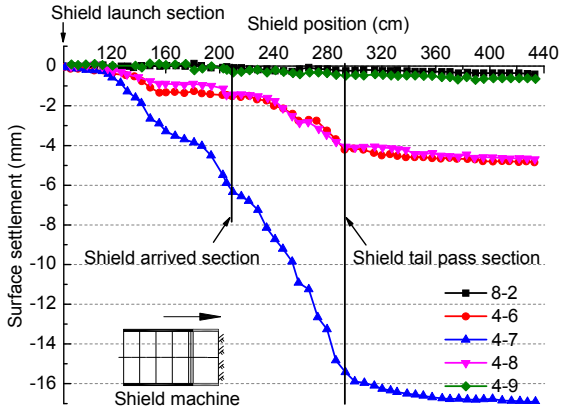

Fig. 9 Surface settlement time-history curve of the left line

Overall, the cross-section settlement curve obtained through model testing was similar to that of the field test. The time-history curves of surface settlement changed at distinct stages. With the shield advancing, the settling trough in the longitudinal section was expanding in the depth direction.

Mair (1997) believed that the fracture shape of the cutting surface in sandy strata is chimney-like, and the fracture shape in cohesive soil is basin-like, deforming moderately in the upper and greatly in the lower strata. The constitution of sandy cobble strata is similar to that of sand strata, so the character of the surface settlement curve should be closer to that of sandy strata. However, the sandy cobble strata had its own property: the settlement curve in sandy cobble strata had a "V" shape, deforming narrowly in the lower strata and expanding in the upper strata. The area of the settling trough was smaller than that of soft ground, similar to that of cohesive soil strata, owing to its discrete property and self-stability.

According to the results of field and model tests, it can be seen that the surface settlement caused by twin-parallel shield tunnelling in sandy cobble strata is different from that in cohesive soil strata. In cohesive soil strata, the deformation of disturbed soil is continuous and follows a gradient, and the affected region of surface settlement caused by shield tunneling is large. However, in sandy cobble strata, the surface settlement curve collapses partially and intermittently. This phenomenon is related to the point-to-point force transmission and self-stability of sandy cobble strata.

Table 4 lists the maximum surface settlement of the three monitoring sections when the cutter arrived

and passed through. The surface settlement rates of each section at different times are listed in Table 5.

Table 4 Maximum surface settlements of each section

Section	Stage	S_{max} (mm)	
		Left line	Right line
Section 1	At the section	−5.21	−5.02
	Past the section	−14.10	−19.02
Section 2	At the section	−6.35	−5.14
	Past the section	−16.58	−19.08
Section 3	At the section	−5.64	−5.47
	Past the section	−15.53	−19.12

Table 5 Surface settlement rate of each section at different times

Stage	Surface settlement rate (%)					
	Right line first			Left line later		
	Section 1	Section 2	Section 3	Section 1	Section 2	Section 3
1D before section	11.1	20.6	19.8	16.4	17.1	16.6
At the section	25.9	17.7	16.5	10.0	9.8	12.0
1D after section	27.2	26.6	26.3	29.7	29.0	28.7
Past the section	35.8	35.1	37.4	43.9	44.0	42.7

According to Table 5, the same conclusion can be drawn from the model test and the field test: most of the surface settlement was caused by the shield gap. However, there are also differences between the tests. The settlement caused by the gap in the model test was 4% (single track) or 14% (double track) larger than that of the field test. Firstly, grouting was not considered in the model test, so the shield tail void was directly filled with ground material, causing the increase in surface settlement. Secondly, the stratum used in the model test was artificial. It was looser and more sensitive to the disturbance caused by shield tunneling, so the surface subsided more after the shield tail passed through the monitoring section.

To describe this difference more clearly, Figs. 10a and 10b show the surface settlement rates of single-track and double-track tunnelings given by the field test and the model test at various stages. The surface settlement rate of the model test was the average of the three monitoring sections. The result for Section 1 was different from those of the other two sections during the first two stages of left line tunneling because of the impact of the shield machine becoming embedded.

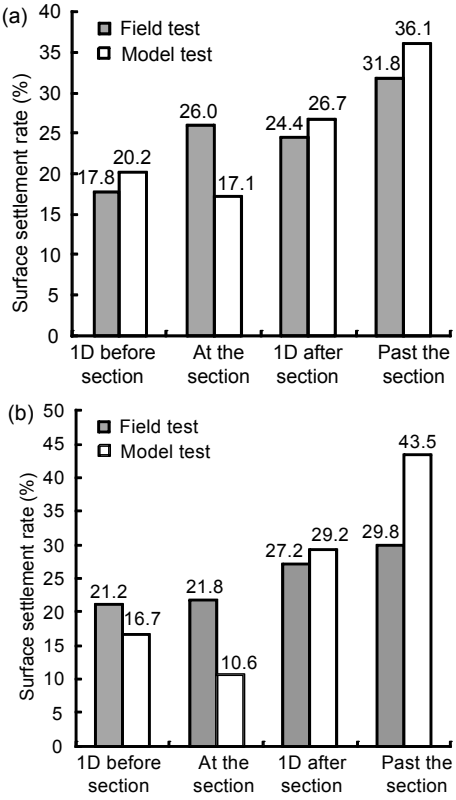

Fig. 10 Surface settlement rates (%) at different times for a single line (a) and a double line (b)

The maximum surface settlement values of each monitoring section obtained by the field test and the model test are listed in Table 6.

Table 6 Maximum surface settlement during shield tunneling

Test			Maximum surface settlement (mm)
Field*		Single track	−13.5
		Double track	−15.1
Model**	Section 1	Single track	−14.1
		Double track	−19.02
	Section 2	Single track	−16.58
		Double track	−19.08
	Section 3	Single track	−15.53
		Double track	−19.12

* Depth 11 m; ** Transformed into an actual depth of 6.5 m

Table 6 shows that the maximum surface settlement during shield tunneling obtained by field testing was less than that of the model test. It may have been affected by the stratigraphic differences and tunnel depth. The overburden of the tunnel in the field test was about 11 m (2D), but in the model test it

was 6.5 m (about 1D). Therefore, it appears that when the overburden reaches a certain extent, a ground arch will occur in sandy cobble strata, and the surface settlement can then be reduced. However, the process cannot be observed in a field or model test, so the mechanism of ground arch formation was examined microscopically using the DEM.

4 Subsidence analysis

Based on field and model tests, this section focuses mainly on the use of the ground loss ratio and surface settlement width to study the influence of twin parallel shield tunnel construction on surface settlement.

4.1 Ground loss ratio

Ground loss is the difference between the actual excavation soil volume and the tunnel completion volume during the shield tunnel construction process (Liu, 1991). Ground loss is used to predict ground deformation in tunnel construction, and the ground loss ratio (the ratio of ground loss to soil excavation area) is often adopted to measure the effect of shield construction on the surrounding environment. There have been few studies of ground loss and its value depends mainly on regional experience. Based on field and model tests, this section studies the relative parameters of ground loss induced by shield tunnel construction in sandy cobble strata.

The transverse surface settlement estimation formula presented by Peck (1969) is as follows:

$$S(x)=S_{\max}\exp[-x^2/(2i^2)], \tag{1}$$

$$S_{\max}=V_{\text{loss}}/(i\sqrt{2\pi}), \tag{2}$$

where x is the transverse distance from the tunnel axis, $S(x)$ is the settlement value at position x, $i=kh$ (O'Reilly, 1982) is the width factor of the settlement trough, k is the width parameter of the settlement trough, h is the overburden of the tunnel, V_{loss} is the ground loss per unit length, $V_{\text{loss}}=\eta\pi R^2$, η is the ground loss ratio, and R is the radius of tunnel.

Based on the surface settlements from field testing, i can be obtained by back-analysis according to Eq. (1). The value of η also can be obtained by back-analysis:

$$\eta=\frac{S_{\max}i\sqrt{2\pi}}{\pi R^2}. \tag{3}$$

Taking into account the impact of secondary soil disturbance on the later tunnel, representative test data from field and model tests have been selected to ensure the accuracy of calculation. Combined with Eqs. (1) and (3), the settlement trough coefficient i and ground loss ratio η in each stage of shield tunneling in sandy cobble strata have been solved (Table 7).

Table 7 Ground loss at different times of shield tunneling

Case	Stage	$S_{\max}$ (mm)	i (m)	η (%)
Field test right line	1D before section	−2.4	2.50	0.05
	At the section	−5.9	3.27	0.17
	1D after section	−9.2	3.43	0.28
	Past the section	−13.5	3.73	0.45
Model test left line (section 2)	1D before section	−3.42	3.66	0.11
	At the section	−6.35	3.76	0.21
	1D after section	−10.76	3.70	0.35
	Past the section	−16.58	3.73	0.55

The back analysis results of settlement trough coefficient i and ground loss ratio η in each stage from the field and model tests are similar (Table 7). The ground loss ratio increases while the shield is advancing. The ground loss in each stage from the field test is smaller than that of the model test as a result of differences between test strata and natural strata.

4.2 Surface settlement trough width

Due to the specific characteristics of sandy cobble strata, the surface settlement scope in sandy cobble strata is smaller than that in soft strata. To illustrate the influence on the scope of surface settlement caused by shield tunneling in sandy cobble strata, representative data from field and model tests were selected (Table 7). Table 8 shows the surface settlement trough width at each stage. Data in the table are the widths of the settlement trough on one side.

Table 8 shows that the surface settlement trough width is related to the shield tunneling stage, and is also influenced by the degree of soil disturbance. Thus, the surface transverse settlement trough expands in the width direction to a certain degree as the shield advances, and the width is distributed mainly within $2.6i$ to $3.1i$. This result could be used as a reference value for soil disturbance induced by shield tunneling in sandy cobble strata.

Table 8 Surface settlement trough width at different times

Content	Stage	i (m)	Surface settlement trough width (m)	Rate with i*
Field test right line	1D before section	2.50	5.7	2.28
	At the section	3.27	10.6	3.24
	1D after section	3.43	10.7	3.12
	Past the section	3.73	11.9	3.19
Model test left line, section 2	1D before section	3.66	9.8	2.68
	At the section	3.76	10.5	2.79
	1D after section	3.70	10.7	2.89
	Past the section	3.73	11.2	3.00

* The ratio of surface settlement tough width and i

5 Numerical analysis

5.1 Particle distinct element

Particle flow code as a simplified distinct method was first proposed by Cundall (1971; 1979) who used it to solve rock mechanics problems. In the particle discrete element world, the properties of particles are studied by simulating the movement and interaction between round granular media. Each particle is treated as a basic element in a whole discrete system, which is based on the finite difference method. The behavior of a discrete group is predicted according to the interaction between particles and the iterative application of Newton's laws of motion at every moment during the whole process.

In the particle-flow model, particles are assumed to be rigid bodies. Contacts occur over a vanishingly small area which can be viewed as a point. Bonds can exist at contact points between particles but a contact bond can transmit only force, not moment, whereas a parallel bond can transmit either. Once a bond is formed at a contact point between two particles, it continues to exist until the inter-particle forces acting at the bond exceed the bond strength, either in the normal or shear way. The constitutive model acting at a particular contact point consists of three parts: the stiffness, slip and bonding models. The stiffness model provides an elastic relation between the contact force and relative displacement. The slip model enforces a relation between shear and normal contact forces such that the two contacting balls may slip relative to each other. The bonding model serves to limit the total normal and shear forces that the contact can carry by enforcing bond-strength limits.

In the particle flow code (PFC) simulation, the interaction between particles is regarded as a dynamic process achieving a static equilibrium when the internal forces are balanced. The dynamic behavior is represented numerically by a time-stepping algorithm using an explicit time difference scheme. Each calculation cycle includes two stages: application of simple interaction laws at particle-particle or particle-wall contacts involving contact forces and relative displacements; and application of Newton's second law of motion to determine the particle motion resulting from any unbalanced forces.

5.2 Parameter calibration

Being different from a continuum model, the micro-parameters in the particle DEM cannot be linked directly to the macro physical and mechanical parameters of materials. To ensure that the numerical model can reflect the expectations of macroscopic physical and mechanical behavior, the connection between some mechanical properties (macroscopic mechanical behavior or response) of the model and the characteristics of a series of associated material parameters (micro-structure mechanics parameters) must be established. Under the premise of fixed particle size and assembly, 2D particle flow code (PFC^{2D}) chooses a biaxial test to establish the link, through a process known as parameter calibration.

Following many years of research on PFC, Zhou (2000; 2006; 2007) summarized the selection criteria for microscopic parameters. Using the existing research results, parameter calibration was carried out for sandy cobble strata. The model was composed of four frictionless walls and particles with specified porosity generated by particle expansion method, and then certain microscopic parameters were set. During the test, a sample loading was simulated by controlling the moving speed of the top and bottom walls. The moving speed of two side walls was controlled by a numerical servo mechanism, making sure the confining pressure was constant. A biaxial test was carried out with three different confining pressures of 0.20 MPa, 0.25 MPa and 0.40 MPa. By changing the parameters in the test process, the microscopic parameters reflecting the characteristics of sandy cobble strata could be obtained (Table 9). Fig. 11 shows the biaxial test specimen. The axial stress-strain curves for different pressures are shown in Fig. 12.

Table 9 PFC parameters of sandy cobble strata after calibration

Density	P (kg/m^3)	R_{max}/R_{min} (m)	μ	K_n (Pa)	K_s (Pa)
Low	2800	0.06/0.08	1	8.0×10^7	8.0×10^7
Medium	3000	0.05/0.06	2	9.8×10^7	9.8×10^7
High	3500	0.09/0.11	6	1.0×10^8	1.0×10^8

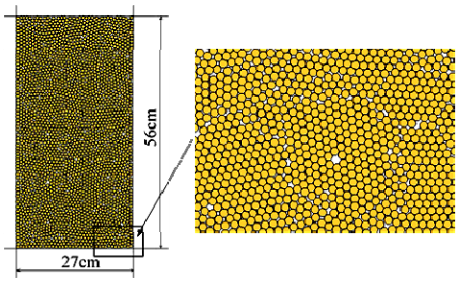

Fig. 11 Particle sample biaxial test

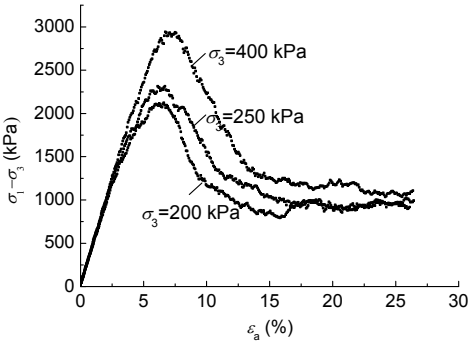

Fig. 12 Axial stress-strain curves with different confining pressures

5.3 Numerical model

Ground changes in the dynamic process of shield advancement cannot be realistically simulated by PFC^{2D}. To achieve the dynamic simulation of shield tunneling, ground loss ratios at different stages obtained above were used in the code, using different ground loss ratios to represent different stages of shield tunneling.

The numerical model must consider the boundary effect and ensure that the analysis results can reflect the relevant characteristics of sandy cobble strata. Thus, the results must be consistent with the field and model test results.

The dimensions of the model were similar to those of the field test. The width×height was 42 m× 24 m and a total of 28 000 particles were generated. The buried depth of the tunnel was 11 m and the diameter of the segment lining was 6 m.

5.4 Analysis results

Taking the single tunnel excavation as an example, the surface settlement trough is shown in Fig. 13 and the maximum settlement in Table 10. The maximum settlement value cannot represent the integrity because of the discrete characteristics, so the average value of the adjacent particles is taken as the maximum value.

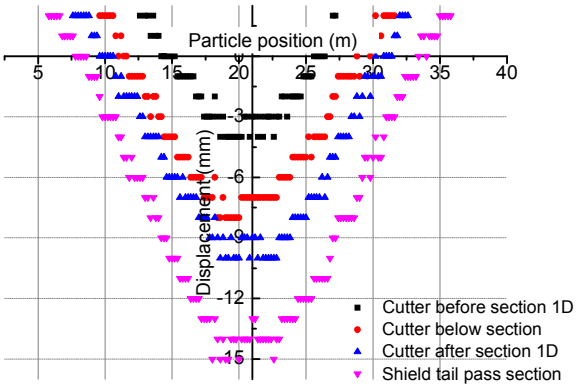

Fig. 13 Surface settlement curve at different time points

Table 10 Maximum settlement of numerical analysis and field test

Method	Maximum settlement (mm)			
	1D before section	At the section	1D after section	Past the section
Numerical analysis	−4.0	−7.0	−10.0	−15.0
Field test	−2.4	−5.9	−9.2	−13.5

Due to the limitation on the extraction accuracy of particle data, the displacement can be determined only to the nearest millimeter, so the particle displacement shows erratic behavior in the surface settlement trough curve.

From the viewpoint of the integrity of the surface settlement curve, the curve and the maximum settlement in each stage are in good agreement with the field test results. This indicates that using the different ground loss ratios to represent different stages of shield tunneling is feasible. This is because the ground loss parameters in PFC^{2D} are back analyzed on the basis of the field test. Therefore, the PFC^{2D} has good applicability in simulating shield construction in sandy cobble strata.

The purpose of numerical simulation was to verify whether a collapsed arch can form on top of a tunnel at different buried depths in sandy cobble strata induced by shield construction disturbance, and to

determine the influence of clear spacing on the formation of such an arch when the buried depth is constant. The analysis cases are shown in Table 11.

Table 11 Numerical analysis cases

Influencing factor	Clear spacing 0.5D	Clear spacing 1.0D	Clear spacing 1.5D	Clear spacing 2.0D
Depth 1.0D	√	√	√	√
Depth 1.5D		√		
Depth 2.0D	√	√	√	√

Because of limited space, in this study we present only four cases: buried depth 1.0D and clear spacing 0.5D, buried depth 1.5D and clear spacing 1.0D, buried depth 2.0D and clear spacing 0.5D, and buried depth 2.0D and clear spacing 2.0D. Figs. 14a–14d show particle contact chains after twin parallel tunnels were excavated.

A collapsed arch gradually forms on top of the tunnel as the buried depth increases from 1.0D to 2.0D (Figs. 14a–14d). When the buried depth is 1.5D, the shape of the arch is obvious. From the perspective of particle movement, owing to the distinct features of sandy cobble strata, the soil particles move to the disturbed zone induced by shield tunneling. When the buried depth is shallow, there are insufficient particles in the disturbed zone to form a collapsed arch, causing the particles to move further into the disturbed zone, and increasing the settlement. When the buried depth is much shallower, particles move and extend to the ground surface, causing surface collapse. When the buried depth reaches a certain level (about 1.5D), the strata porosity decreases and coordination number increases due to the effects of friction resistance and gravity in the process of the movement of particles to the disturbed zone. This creates a mutual wedge between the particles, and hence a collapsed arch forms on top of the tunnel.

The clear spacing between two tunnels had a major impact on the formation of a collapsed arch. When the spacing was small (about 0.5D), the collapsed arch crossed above the two tunnels and formed a large arch (Fig. 14c). As the spacing increased, the large arch gradually expanded into two separate smaller arches. When the spacing was 2.0D, there were two independent collapsed arches on top of each tunnel (Fig. 14d), and the influence of the other tunnel could be ignored. Therefore, the designed buried depth and clear spacing between two tunnels play an important role in controlling surface deformation in sandy cobble strata.

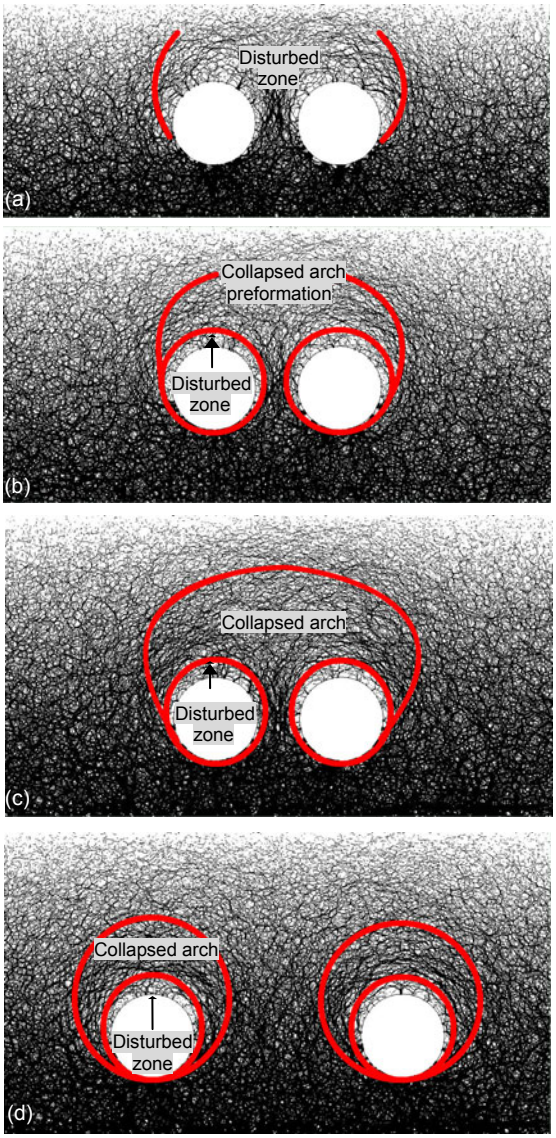

Fig. 14 Particle contact force chain with (a) 1.0D buried depth and 0.5D clear spacing; (b) 1.5D buried depth and 0.5D clear spacing; (c) 2.0D buried depth and 0.5D clear spacing and (d) 2.0D buried depth and 2.0D clear spacing

6 Discussion and conclusions

Sandy cobble strata can easily be disturbed by shield tunneling. A field test, model test and particle distinct element method were carried out to study the soil disturbance caused by shield tunneling in sandy cobble strata. Some conclusions can be drawn as follows:

1. The shape of the surface transverse settlement curve caused by shield tunneling in sandy cobble strata is a deep V-shape, and the surface settlement time-history curve presents mutability. The surface deformation zone caused by shield tunneling in sandy cobble strata is smaller than that in soft strata. The construction gap is the key reason for ground loss caused by shield tunneling.

2. The trends in the surface settlement trough width coefficient and ground loss ratio are basically consistent during the advance of the shield in sandy cobble strata, and then increase to a certain value. The surface settlement trough width caused by shield tunneling distributes within $2.6i$–$3.1i$.

3. Particle discrete element method has good applicability for the simulation of shield construction in sandy cobble strata. When the buried depth is greater than 1.5D, soil particles in the disturbed zone can form a collapsed arch on top of the tunnel, reducing the surface settlement effectively. When the clear spacing between two tunnels is greater than 2.0D, an independent collapsed arch can form.

A model test was carried out by using an independently designed EPB shield machine. Due to limitations in the size of the model machine, gravel particles were not used. Rather, model soil with similar controlling parameters to the natural strata was tested. Further work is needed to design a larger model machine to consider the presence of gravel particles.

References

Chen, S.L., Li, G.W., Gui, M.W., 2009. Effects of overburden, rock strength and pillar width on the safety of a three-parallel-hole tunnel. *Journal of Zhejiang University-SCIENCE A*, **10**(11):1581-1588. [doi:10.1631/jzus.A0920040]

Cundall, P.A., 1971. A Computer Model for Simulating Progressive Large Scale Movements in Blocky Rock System. Proceedings of International Symposium on Rock Mechanics, Rock Fracture, Nancy, France, p.2-8.

Cundall, P.A., Strack, O.D.L., 1979. A discrete numerical model for granular assemblies. *Geotechnique*, **29**(1): 47-65. [doi:10.1680/geot.1979.29.1.47]

Lee, K.M., Rowe, R.K., Lo, K.Y., 1992. Subsidence owing to tunnelling I: estimating the gap parameter. *Canadian Geotechnical Journal*, **29**(6):929-940. [doi:10.1139/t92-104]

Liu, J.H., Hou, X.Y., 1991. Shield Tunelling Method. China Railway Publishing House, Beijing, p.329-332 (in Chinese).

Loganathan, N., Poulos, H.G., 1998. Analytical prediction for tunneling induced ground movements in clays. *Journal of Geotechnical and Geoenvironmental Engineering*, **124**(9):846-856. [doi:10.1061/(ASCE)1090-0241(1998)124:9(846)]

Lo, K.Y., Ng, R.M.C., Rowe, R.K., 1984. Predicting Settlement due to Tunnelling in Clays. Tunnelling in Soil and Rock, American Society of Civil Engineers, Geotech III Conference, Atlanta, USA, p.46-76.

Mair, R.J., Taylor, R.N., 1997. Theme Lecture: Bored Tunneling in the Urban Environment. 14th International Conference on Soil Mechanics and Foundation Engineering, Rotterdam, p.2353-2358.

O'Reilly, M.P., New, B.M., 1982. Settlements above Tunnels in the UK: Their Magnitude and Prediction. Proceedings of Tunnelling Symposium, London, p.173-181.

Peck, R.B., 1969. Deep Excavations and Tunnelling in Soft Ground. 7th International Conference on Soil Mechanics and Foundation Engineering, Mexico City, Mexico, p.225-290.

Rowe, R.K., Lo, K.Y., Kack, G.J., 1983. A method of estimating surface settlement above tunnels constructed in soft ground. *Canadian Geotechnical Journal*, **20**(1):11-22. [doi:10.1139/t83-002]

Itasca Consulting Group, 2004. PFC2D (Particle Flow Code in 2 Dimensions), Version 3.1. User's Manual. Minneapolis.

Sagaseta, C., 1987. Analysis of undrained soil deformation due to ground loss. *Geotechnique*, **37**(3):301-320. [doi:10.1680/geot.1987.37.3.301]

Sagaseta, C., 1988. Discussion on 'Analysis of undrained soil deformation due to ground loss' by C. Sagaseta. *Getechnique*, **38**(4):647-649. [doi:10.1680/geot.1988.38.4.647]

Uriel, A.O., Sagaseta, C., 1989. Selection of Design Parameters for Underground Construction. 12th International Conference on Soil Mechanics and Foundation Engineering. Rio de Janeiro, Balkema, p.2251-2551.

Verruijt, A., Booker, J.R., 1996. Surface settlements due to deformation of a tunnel in an elastic half plane. *Getechnique*, **46**(4):753-756. [doi:10.1680/geot.1996.46.4.753]

Wei, G., 2007. Prediction of surface settlement induced by ground loss during shield tunneling construction. *Rock and Soil Mechanics*, **28**(11):2375-2379 (in Chinese).

Wei, G., 2009a. Prediction of ground deformation induced by shield tunneling construction. *Chinese Journal of Rock Mechanics and Engineering*, **28**(2):418-424 (in Chinese).

Wei, G., 2009b. Study on calculation for width parameter of surface settlement trough induced by shield tunnel. *Industrial Construction*, **39**(12):74-79 (in Chinese).

Wei, G., 2010. Selection and distribution of ground loss ratio induced by shield tunnel construction. *Chinese Journal of Geotechnical Engineering*, **32**(9):1354-1361 (in Chinese).

Zhou, J., Ci, Y.W., Ci, Y., Xu, J.P., 2000. Simulation of biaxial test on sand by particle flow and code. *Chinese Journal of Geotechnical Engineering*, **22**(6):701-704 (in Chinese).

Zhou, J., Su, Y., Ci, Y., 2006. Simulation of soil properties by particle flow code. *Chinese Journal of Geotechnical Engineering*, **28**(3):390-396 (in Chinese).

Zhou, J., Kong, X.L., Ju, Q.H., Li, Y.Q., 2007. Mesoscopical study on interface between geosynthetics and soil. *Chinese Journal of Rock Mechanics and Engineering*, **26**(1): 3196-3202 (in Chinese).